

Carbon nanotubes and nanofibres

Bojan O. Boskovic^{1,2,3,*}

¹*Dunlop Aerospace Braking Systems, Meggitt PLC, Holbrook Lane, Coventry, CV6 4AA, UK*

²*Department of Materials Science & Metallurgy, University of Cambridge, Cambridge, CB2 3QZ, UK*

³*School of Applied Sciences, Cranfield University, Cranfield, Bedfordshire, MK43 0AL, UK*

1. Introduction

A carbon nanotube (CNT) is a tubular carbon structure with hollow cylindrical graphene walls comprised of hexagonally arranged sp^2 -bonded carbon atoms parallel to the longitudinal axis, capped by fullerene-type hemispheres. The carbon nanotube with a single graphene tube (Fig. 1) is called a single wall carbon nanotube (SWCNT). A multi-wall carbon nanotube (MWCNT) consists of a number of concentric graphene tubes (of different diameters) nested within each other like the “Russian” nested dolls called Matryoshka (also known as Babushka). Other carbon structures with herringbone or cup-stacked graphene layers, which form an angle with the longitudinal axis, are referred to as carbon nanofibres (CNFs).¹ The carbon nanotube diameter could vary from only a few nanometres for SWCNTs up to few tens of nanometres for MWCNTs and more than a hundred nanometres for CNFs, and the length could vary from microns up to millimetres and even centimetres.

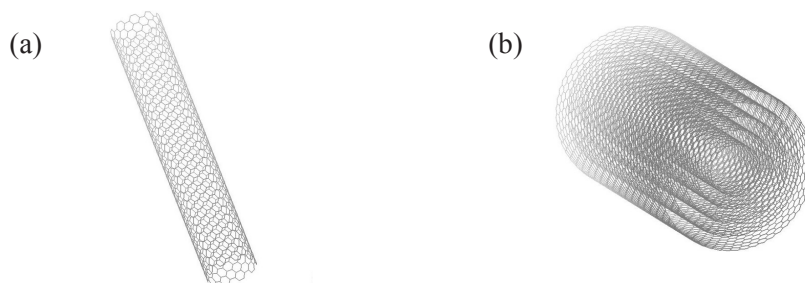


Figure 1. (a) A single graphene layer rolled into a tube as an illustration of the single wall carbon nanotube structure; (b) concentric graphene tubes of different diameters nested within each other like “Russian” dolls, illustrating a multiwall carbon nanotube structure. (Courtesy of Jane Crawshaw.)

* E-mail: bob23@cam.ac.uk, b.o.boskovic@cranfield.ac.uk

¹ Carbon nanofibres (CNF) is now the accepted term covering all filamentous structures other than the strictly ordered single- and multiwall carbon nanotubes (CNT). Typically nanofibres have a defective or irregular graphene layer structure.

Carbon nanotubes and nanofibres (filaments) have been made successfully for more than two decades using a method known as chemical vapour deposition (CVD). In the CVD of carbon nanomaterials, a hydrocarbon gas is passed over a heated catalyst. The actions of the catalyst cause the hydrocarbon to decompose into hydrogen and carbon atoms, which provide the feedstock for the carbon nanofibre/nanotube growth. Carbon nanofibres and nanotubes grown by the CVD method usually have catalyst particles attached to one end. Multiwalled nanotubes grown this way tend to have a large number of structural defects.

Nanotubes can behave like metals or semiconductors, can conduct electricity better than copper, can transmit heat better than diamond, and rank among the strongest materials known. The electronic properties of the resulting nanotube depend on the direction in which the graphene sheets were rolled up. Some nanotubes behave like metals with high electrical conductivity, while others behave like semiconductors with relatively large band gaps.

In the last two decades carbon nanotube- and nanofibre-related research and development has grown considerably, both in academia and industry. The development of new production routes, and the prediction and observation of unusual properties, has led to the suggestion and realization of many fascinating applications. Carbon nanotube and nanofibre development has already attracted a large amount of effort from hundreds of research groups around the world and it is growing rapidly. In this article, a historical overview of carbon nanotube and nanofibre research and development together with the most popular synthesis methods and the most recent discoveries and applications will be presented.

2. A short history

The formation of carbon filaments from the interaction of gases containing carbon with hot metal surfaces has been known since the end of 19th century. Hughes and Chambers patented the manufacture of carbon filaments in 1889 [1]. They described hair-like carbon filaments that may be bent and twisted into various shapes and will spring back to their original form when released. The filaments were formed directly from a gas capable of yielding carbon by decomposition when placed in a crucible of plumbago or iron in a furnace at high temperature. Paul and Léon Schützenberger in 1890 [2] found that filaments were deposited when cyanogen was passed over porcelain at “cherry-red” temperature.

Individual carbon filaments were first observed when electron microscopy came into widespread use around 1950 [3, 4]. Radushkievich and Luk’yanovich reported the first electron micrograph of carbon filaments in 1952 [3]. Davis et al. in 1953 published the first English language paper with electron micrographs of carbon filaments [4]. The motivation for Davis and his co-workers’ research work was the prevention of carbon deposition in the brickwork of blast furnaces, because carbon deposition may cause disintegration of the bricks. They found that carbon is formed by the interaction of carbon monoxide and iron oxide in the so-called iron spots in the brick. By exposing samples of brick containing iron spots to the carbon monoxide at an optimal temperature of about 450 °C, they produced carbon filaments (similar to carbon nanofibres). The nanofibres had catalyst particles located at the tip and some of them exhibited a helical form.

In the 1970s and 1980s two opposing interests motivated research into the properties and mechanisms of carbon filament (nanofibre) growth: the inhibition of carbon filament growth

and the optimization of carbon filament growth. The prevention of carbon deposition is a high priority for many processes involving hydrocarbon conversion reactors. Here the presence of such nanostructures creates problems, including blockage of reactors, reduction of heat transfer properties and deactivation of catalyst systems due to encapsulation of the metallic components [5]. Then in 1985 the discovery of the C_{60} molecule (also known as buckminsterfullerene, one of the fullerene family) was reported by Kroto et al. [6], which marked the beginning of a new era in carbon and science.

In 1991, Sumio Iijima, using high-resolution transmission electron microscopy at the NEC in Tsukuba, Japan, reported the first observation of structures that consisted of several concentric tubes of carbon nested inside each other, like the Russian dolls [7]. He called them microtubules of graphitic carbon, but from 1992 onwards Iijima and other researchers began to call them carbon nanotubes. Iijima observed MWCNTs in the soot produced by an electric arc discharge between graphite electrodes in a helium atmosphere. Subsequently, in 1993, Iijima and Ichihashi at NEC [8] and Bethune and co-workers at IBM [9] independently discovered SWCNTs. Diameters of single-wall nanotubes were just one or two nanometres, compared to MWCNT diameters, which are of the order of tens of nanometres. In subsequent years a great deal of research effort was invested to find efficient methods of producing large quantities of nanotubes. In 1992, Ebbesen and Ajayan, also at NEC, developed a method of producing larger quantities (a few grams) of high-quality MWCNTs by vaporizing carbon electrodes [10]. Since then other carbon nanotube synthesis methods have been developed. Carbon nanotubes have been produced by vaporizing a graphite target using a laser [11, 12], electron beam [13], and solar energy [14] sources. Catalytic chemical vapour deposition (CVD) of hydrocarbons [15] is now widely used for carbon nanotube synthesis; it is a simple and efficient method.

Applications of carbon nanotubes and nanofibres are now attracting considerable interest from both the academic and the industrial communities. Carbon nanotubes have proven to be good field emitters [16–20], scanning electron microscope tips [21], conducting fillers in polymer-based composite materials [22], and useful in fuel cells [23]. They can be used in nanoelectronics as diodes and transistors [24], in supercapacitors [25], as electromechanical actuators [26], as chemical sensors [27], as cell growth scaffolds [28], in DNA microarrays [29], and for protein sensing [30].

3. Structure

Iijima in 1991 [7] published the first electron microscopy image of multiwalled carbon nanotubes with graphene layers parallel to the nanotubes axis. Experimental observation of a carbon nanotube with a diameter corresponding to that of a C_{60} molecule was reported in 1992 by Ajayan and Iijima [31]. A single wall C_{60} -derived carbon nanotube consists of a bisected C_{60} molecule with the two resulting hemispheres joined together by a cylindrical tube one monolayer thick and with the same diameter as C_{60} . If the C_{60} molecule is bisected normal to the five-fold axis, the “armchair” nanotube is formed, and if the C_{60} molecule is bisected normal to the threefold axis, the zigzag nanotube is formed [32]. In addition to armchair and zigzag nanotubes, a large number of chiral nanotubes can be formed with a screw axis along the axis of the nanotube and a variety of hemispherical-like caps. Armchair and zigzag carbon nanotubes with larger diameters have correspondingly larger caps. Structures with smaller caps, for

example C_{36} , with a diameter of 0.5 nm [33], and C_{20} , with a diameter of 0.4 nm, have been reported [34, 35].

The first researchers who reported carbon nanofibre formation [3, 4] established that carbon nanofibres had metal particles associated with them. Catalytic ‘ice cream cone’ or heart-shaped metal particles can usually be seen at the end of the nanofibre. Alternatively, diamond-shaped metal catalyst particles can sometimes be seen in the middle of the nanofibres.

Detailed investigation of carbon nanotube structures by high-resolution electron microscopy has revealed that the carbon nanotube consist of a cylindrical arrangement (Fig. 2). The central part of the carbon nanofibre is less dense (more electron-transparent) than the outer region of the tube, which shows well ordered regions of individual graphite platelets. The graphite platelets are usually aligned parallel to the side faces of the catalyst particle.

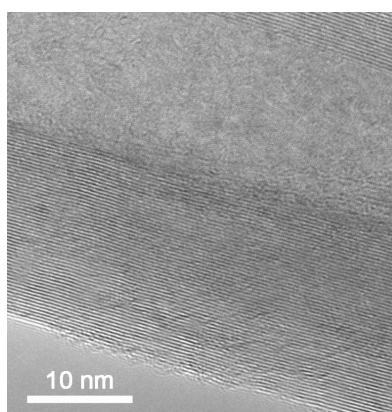


Figure 2. HRTEM image of a multiwall carbon nanotube with graphene layers parallel to its axis. (Courtesy of Krzysztof Koziol.)

Baird, Fryer and Grant [36, 37] studied the effects of heating nickel foil to 600 °C in methane or propane and identified carbon nanofibres among other carbonaceous deposits. They have performed a detailed investigation of carbon nanofibre structures by high resolution transmission electron microscopy (HRTEM) and revealed the 0.34 nm interlayer spacing of graphite. They showed that at the nanofibre tips, the basal plane layers were parallel to the surface of the metal catalyst.

Further HRTEM studies by Rodriguez, Chambers and Baker [38] have shown that the nanofibres consist of a well ordered graphite platelet structure, the arrangement of which can be engineered to the desired geometry by choice of the correct catalyst system. Depending on the chemical nature of the catalyst and the conditions of the reaction, assorted nanofibre structures with various morphologies and different degrees of crystallinity can be produced. Nanofibres consist of graphite platelets that can be oriented in various directions with respect to the fibre axis.

In addition to the whisker-like carbon nanofibre structure, several other morphologies have been found, including bidirectional, helical, branched and coiled. Tubes (hollow cored structures), bitubes (with the catalyst particle enclosed), solid structures and shells were also observed.

Davis et al. [4] reported coiled (helical) carbon fibres for the first time in 1953. Motojima et al. [39] have obtained very large coiled carbon fibres using acetylene at temperatures ranging from

400 to 550 °C at atmospheric pressure with Ni powder and single crystal Ni plates as catalyst materials. It was apparent that they had grown these coiled fibres via a bidirectional mode, with the diamond-shaped catalyst particle contained within the body of the nanofibre.

A common feature for all these structures is that the width of the nanofibre is determined by the size of the associated catalyst particle. Bernardo et al. [40] reported different structures, with various nanofibres attached to the same catalyst particle, which was much larger than the nanofibres in width. They named this structure “octopus carbon”.

Thess et al. [41] reported the first synthesis of crystalline ropes of metallic SWCNTs in 1996. They produced SWCNTs that were nearly uniform in diameter and self-organized into ‘ropes’, which consist of 100 to 500 SWCNTs, by the condensation of laser-vaporized carbon-nickel-cobalt mixtures at 1200 °C. They estimated that typically 70 to 90% of the material was SWCNT ropes, and the ends of the ropes could not be found in the TEM images due to their long length.

Long and wide ropes of SWCNT bundles with rope diameters of 100 µm and lengths up to 3 cm, synthesized by the catalytic decomposition of hydrocarbons, were described by Cheng et al. [42].

The carbon ropes with diameters on the micrometre scale cannot be observed by TEM in their as-prepared state. Vigorous ultrasonic dispersion is needed to prepare the samples for observation, which destroys the original structure, notably the alignment and their interrelationships. TEM observations cannot reflect the original bundle construction exactly, but many long SWCNTs in small bundles and individual tubes released from the carbon ropes could be observed.

Many groups have been making fibres from carbon nanotubes. Usually these fibres are made by drawing from a mixture of nanotubes and polymer like polyvinyl alcohol as demonstrated by Dalton et al. [43], or from nanotubes dispersed in sulfuric acid as shown by Davis et al. [44]. Zhang et al. [45] reported that fibres can also be drawn from aligned carpets/arrays of nanotubes. Nanotubes in all these fibres are relatively short; therefore the fibre strength is based on local entanglement between nanotubes, as in typical cotton-type fibres. However, the most elegant and simplified way of making continuous fibres consisting of pure nanotubes was reported by Li et al. [46]: the so-called direct spinning method, from a CVD reactor. It was found that single and double wall nanotubes, in the form of bundles, were present in these fibres. The nanotubes were extremely well aligned and very long, therefore it was not possible to find any nanotube ends. They can also be twisted into a variety of forms.

4. Synthesis

The first carbon nanotubes identified by Iijima in 1991 were synthesized using a carbon arc discharge [7]. Since then a number of other methods of carbon nanotube growth have been developed, including vaporizing a graphite target using a laser [11, 12], and electron beam [13] sources. In addition, the production of relatively imperfect carbon nanotubes by catalytic chemical vapour deposition methods at high temperatures has been known for decades [4].

Flow of a reactant gas containing carbon over a transition metal catalyst results in the synthesis of carbon nanotubes and nanofibres. This process is known as chemical vapour deposition (CVD). It has two main advantages. Firstly, the nanotubes are obtained at a much lower temperature compared with other methods; however this can be at the cost of structural quality. Secondly, the catalyst can be grown on a substrate, which allows growth of aligned

nanotubes and control of their growth. Nanotubes can be grown on surfaces with a degree of control that is unmatched by arc discharge or laser ablation techniques. The defective nature of CVD-grown MWCNT remains poorly understood. This may be due to the relatively low temperatures that are used, which do not allow the nanotube walls to fully crystallize.

Intensive research into the catalytic formation of carbon filaments (now known as nanofibres) began in the 1970s. The work of Baker and his colleagues [47], and other researchers in the 1970s and 1980s, proceeded in opposite directions—attempting to inhibit carbon nanofibre growth and optimize growth. Research into inhibiting carbon nanofibre growth was motivated by the fact that the presence of such filaments could constitute a serious problem in certain chemical processes, as well as in the operation of gas-cooled nuclear reactors. As a result of the huge interest in carbon nanotubes in the 1990s, catalytic carbon nanotube synthesis methods have been under intense research activity to produce large quantities of this material. Jose-Yacaman et al. [48] have concluded that catalytic methods can produce carbon nanotubes with very similar characteristics to those from the carbon-arc method.

The catalytic CVD method is now regarded, in both the scientific and business communities, as the best method for cheap and efficient production of large quantities of carbon nanotubes. Carbon nanotubes produced by this method have more structural defects compared to nanotubes produced by arc discharge [7, 10, 49] or laser vaporization [47, 50]. However, a perfect carbon nanotube structure is not crucial for many applications. The key parameters involved in growing nanotubes using CVD are the types of hydrocarbons and catalysts used, and the temperature at which the reaction takes place.

In the 1998 Hongjie Dai group at Stanford University succeeded in producing single-wall nanotubes with perfect structures for the first time using CVD [51]. Their approach used methane gas as the carbon source and temperatures in the range of 900–1000 °C. Such high temperatures are needed to form single-walled nanotubes that have small diameters and high strain energies, and to produce virtually defect-free tubes.

Current synthesis of carbon nanotubes using a thermal CVD process or the catalytic pyrolysis of hydrocarbons is very similar to methods used for carbon nanofibre production, developed and studied in the 1970s in 1980s by Baker and others [52]. Catalytically-produced carbon nanotubes using a CVD process are similar to the CARBON FIBRILS™ patented by Hyperion Catalysis International [53].

A method was also presented by Singh et al. [54] to produce high purity, aligned multi-walled carbon nanotube films grown on thin quartz flakes by injecting a solution of ferrocene in toluene into a tube furnace. After reaction, these quartz flakes support arrays of nanotubes arranged perpendicular to the surfaces of the substrate. This method is seen to increase the yield of nanotubes dramatically compared to the conventional injection CVD method.

Carbon nanotubes and nanofibres can be synthesized using plasma-enhanced CVD (PECVD), where the hydrocarbon gas is in an ionized state above the transition metal catalyst (nickel, iron, cobalt, etc.). The electrical (self-bias) field from plasma can be sufficient to induce aligned CNT growth perpendicular to the substrate. The PECVD method can use different energy sources for creation of the plasma state, and allows lower deposition temperatures than thermal CVD. Hot filament PECVD uses thermal energy for plasma creation and has been used successfully for carbon nanotube production by Ren and co-workers [17]. Microwave PECVD

has also been successfully used in the production of carbon nanotubes and nanofibres [55–59]. Synthesis of vertically aligned CNTs and CNFs requires the application of an electric field normal to the substrate, and DC PECVD is the most suitable method to achieve this [60, 61]. Inductively coupled plasma PECVD [62, 63] and radio frequency PECVD [64, 65] methods have also been used successfully for carbon nanotube and nanofibre synthesis. Ren et al. in 1998 [17] reported the first successful growth of large scale, well aligned carbon nanofibres on nickel foils and nickel-coated glass at temperatures below 660 °C. Acetylene gas was used as the carbon source and mixed with ammonia in a plasma-enhanced hot filament chemical vapour deposition (PE-HFCVD) system. They concluded that plasma intensity, acetylene to ammonia gas ratio and their flow rates affect the diameter and uniformity of the carbon nanofibres. A spherical particle of Ni was found on the tip of each nanofibre. Bower et al. [58] have grown well aligned carbon nanotubes using microwave PECVD with the addition of a radio frequency graphite heater. They found that switching off the plasma source effectively turns off the alignment mechanism, leading to the thermal growth of curly nanotubes. Merkulov et al. [60] reported synthesis of vertically aligned CNFs on patterned catalyst using DC PECVD with acetylene (C₂H₂), ammonia (NH₃) and helium (He). The catalyst patterns were fabricated using conventional electron beam lithography. The ammonia was used to etch away the amorphous carbon (a-C) film that was continuously formed during the growth. The shape of CNFs depends on the growth rate at the tip by catalysis and the deposition rate of a-C from the plasma along the sidewalls [66]. This ratio is controlled by the catalyst activity, and by the balance of deposition and etching of a-C, which in turn depends on the plasma, the etchant (NH₃) and the hydrocarbon gas (C₂H₂). This balance has been studied by Merkulov et al. [60] and Teo et al. [67]. The PECVD method allows growth of carbon nanotubes and nanofibres at relatively low temperatures, making it suitable for temperature-sensitive substrates. A radio frequency PECVD carbon nanofibre synthesis at room temperature has been reported by Boskovic et al. [65]. Using DC PECVD Hofmann et al. [68] demonstrated synthesis of aligned carbon nanofibres at temperatures as low as 120 °C and on plastic (polymer) substrates [69].

Successful synthesis of carbon nanofibres (filaments) in the 1970s led to the question of growth mechanisms and the role of the catalytic particles. A few growth models were proposed, by Baker et al. [70, 71] and Oberlin et al. [72]. These models have been adopted for carbon nanotube CVD growth. However, a complete mechanism, which can explain the various, and often conflicting, data has yet to be proposed.

Baker et al. in 1972 [70] developed the most influential model for carbon nanofibre growth, based on direct growth observations using controlled atmosphere microscopy and the assumption that diffusion flow was primarily driven by the temperature gradient. Helveg et al. in 2004 [73] presented evidence for the carbon nanofibre growth mechanism obtained using time resolved, high resolution *in situ* TEM observation of the formation of carbon nanofibres from methane decomposition over supported nickel nanocrystals. Carbon nanofibres were observed to develop through a reaction-induced reshaping of the nickel nanocrystals. The nucleation and growth of graphene layers was found to be assisted by dynamic formation and restructuring of monoatomic step edges at the nickel surface.

The key parameters involved in nanotube growth using CVD are the types of hydrocarbons and catalysts used, and the temperature at which the reaction takes place. Most of the CVD

methods used to grow multiwalled carbon nanotubes and nanofibres use methane, ethylene or acetylene gas as the carbon feedstock, and iron, nickel or cobalt nanoparticles as the catalyst. Transition metals, such as iron, nickel and cobalt are well known to be active catalysts, but the exact mechanism of their action is still uncertain. Reactions with hydrocarbons are favoured by the presence of hydrogen, and oxides can also help. For experiments with iron catalysts, some authors claim that the active catalyst could be iron carbide: Fe_7C_3 , FeC or Fe_3C . The growth chamber temperature is typically in the range of 650 to 750 °C for thermal CVD and much lower for PECVD. The hydrocarbon dissociates on the metal nanoparticles, and the resulting carbon then diffuses across it, which eventually becomes saturated. The carbon then precipitates to form solid carbon tubes, the diameters of which are determined by the size of the metal catalyst particles. The interaction between the metal catalyst particle and the supporting medium is a further factor that influences the nanofibre and nanotube growth characteristics. A weak interaction results in a “tip growth” model where a catalyst particle is lifted off the support and onto the tip of the CNT/CNF. A strong interaction results in growth by the extrusion mode or the “base” or “root” growth mechanism, in which the catalyst particles remain attached to the support.

5. Properties

Due to the high aspect ratio, the quasi-one-dimensional structure, and the graphite-like arrangement of the carbon atoms in the shells, nanotubes exhibit a very broad range of unique chemical, mechanical and electronic properties. The properties of nanotubes can change depending on their different structures (defined by the diameter, length, and chiral angle) and quality (defined by defect concentration). The nanometre size of CNTs provides a high specific surface, which depends on the diameter of the nanotube, and is the highest for the smallest diameter SWCNTs. Large increases in strength and toughness, and superior electrical/thermal properties are the potential benefits of using nanotubes as the filler material in polymer-based composites when compared with traditional carbon, glass or metal fibres. The remarkable electrical and mechanical properties of carbon nanotubes make them excellent candidates for a range of electrical, mechanical and electromechanical applications. A review of carbon nanotube properties is given in ref. [74].

The unusual electronic structure of a graphene layer made up of sp^2 -bonded carbon atoms is the origin of the remarkable electronic properties of carbon nanotubes. These properties depend on the direction in which the graphene sheet is rolled up, the so-called chirality. Before measuring the conducting properties of nanotubes it is necessary to attach metal electrodes to them. The electrodes, which can be connected to either a single tube or a bundle of up to several hundred tubes, are usually made using electron-beam lithography. The tubes can be attached to the electrodes in a number of different ways. One way is to create an electrode on a substrate and then drop a dilute dispersion of the tubes onto the electrode. Another is to deposit the tubes onto a substrate, locate them using a scanning electron microscope (SEM) or atomic force microscope (AFM), and then deposit leads to the tubes using lithography.

More advanced techniques are also being developed to improve reproducibility and control in device fabrication. These include the possibility of growing the tubes between the electrodes. In semiconducting materials, a small amount of impurity added as a dopant can make it n-type or p-type. A junction between a p- and an n-type semiconductor acts as a diode. A junction can

also be formed between a semiconductor and a metal. Carbon nanotubes can be either metallic or semiconducting, depending on their chirality. Hence, experimentally observed diode properties can be explained by the presence of a junction between two electronically differing nanotubes [75]. Carbon nanotubes have shown p-type semiconductor behaviour. One might expect an isolated semiconducting nanotube to be an intrinsic semiconductor, in which excess electrons are created by thermal fluctuations alone. However, it is now believed that the metal electrodes, as well as chemical species absorbed on the tube, dope the tube p-type. In other words, they remove electrons from the tube, leaving the remaining mobile holes responsible for conduction. Lieber et al. [76] carried out one of the first conductivity measurements of individual nanotubes. To measure the electrical properties of an individual carbon nanotube, they deposited a drop of a nanotube suspension onto a flat insulating surface and covered it with a uniform layer of gold. A conducting cantilever in the AFM made it possible to establish electrical contacts and measure the axial conduction through a single nanotube to the gold contacts whilst simultaneously imaging the nanotube structure. Measurements were taken on catalytically-grown MWCNTs with diameters of 8.5 nm and 13.9 nm, and their resistance per unit length was $0.41 \text{ M}\Omega/\mu\text{m}$ and $0.06 \text{ M}\Omega/\mu\text{m}$ respectively. In order to avoid possible ambiguities due to poor sample contacts, Ebbesen et al. [77] have developed a four-probe measurement method on single nanotubes by lithographic deposition of tungsten leads across the nanotubes. They found that each MWCNT has unique conductivity properties and that differences between the electrical properties of different nanotubes were far greater than expected. Both metallic and semiconducting behaviour was observed on arc-grown SWCNTs. However, they found that the majority of tubes are essentially metallic in nature.

The conductivity of an individual SWCNT was studied by Tans et al. [79]. Because of the structural symmetry and stiffness of SWCNTs, their molecular wave functions may extend over the entire tube. These researchers have found that electrical transport measurements on individual SWCNTs confirm theoretical predictions and that they appear to behave as coherent quantum wires. Electrical conduction seems to occur through well-separated, discrete electron states that are quantum-mechanically coherent over long distances of at least 140 nm from contact to contact. The two-point resistance at room temperature of a single tube was generally found to be around $1 \text{ M}\Omega$. Traditional electronic devices are based on classical electron diffusion. The size of the devices, at nanometre level, becomes comparable to the electron coherence length and quantum interference between electron waves starts to influence device properties. Carbon nanotubes are promising candidates to exploit quantum effects for the benefit of future nanoelectronic devices. Experimental [79–89] and theoretical studies [75, 79, 90] have indicated that carbon nanotubes behave as one-dimensional ballistic conductors with quantized conductance. When the length of the conductor is smaller than the electron mean free path, then electron transport is ballistic [90, 91], in which case there is no energy dissipation in the conductor and the Joule heat is dissipated in the electrical leads that connect the ballistic conductor to the elements of the circuit.

The first report of SWCNT rope synthesis by Colbert et al. [92] also described the first measurement of the electrical properties of ropes of SWCNT. They measured the electrical resistivity of a single rope using a four-point technique; values for different ropes ranged from 0.34×10^{-4} to $1 \times 10^{-4} \Omega \text{ cm}$. Bockrath et al. [81] observed dramatic peaks in the conductance as

a function of the gate voltage that modulated the number of electrons in the rope. They interpreted these results as the effect of single electron charging and resonant tunnelling through the quantized levels of the nanotubes composing the rope. Intertube conductance inside the rope was low compared to the conductance along the tube.

In a sheet of graphite each carbon atom is strongly bonded to three other atoms, which makes graphite very strong in certain directions. However, adjacent sheets are only weakly bonded by van der Waals forces. Layers of graphite can be easily peeled apart, as happens when writing with a “lead” pencil, but it is not easy to peel a carbon layer from a multiwalled nanotube. Carbon fibres have already been used to strengthen a wide range of materials, and the special properties of carbon nanotubes mean that they could be the ultimate-strength fibre. The remarkable mechanical properties of carbon nanotubes are already exploited as tips in scanning probe microscopes. Since they are composed entirely of carbon, nanotubes also have a low specific weight. Nanotubes also offer great promise as the active elements in nanoelectromechanical systems. Their remarkable mechanical and electronic properties make them excellent candidates for applications such as high-frequency oscillators and filters.

In 1996, Treacy et al. [92] investigated elastic stiffness and measured the Young’s modulus of multiwalled nanotubes. They arranged multiwalled nanotubes vertically on a surface so that the tubes were fixed at the bottom and free to move at the top, and then used a transmission electron microscope (TEM) to measure the thermal vibration frequency of the free ends. The measured vibration amplitude revealed an exceptionally high Young’s modulus of 10^{12} N/m², about five times the value for steel. The carbon-carbon bonds within the individual layers mainly determine the Young’s modulus. Salvetat et al. [94] found that multiwalled nanotubes grown by arc discharge had a modulus of one or two orders of magnitude greater than those grown by catalytic CVD of hydrocarbons. These results demonstrate that only highly ordered and well-graphitized nanotubes have a stiffness comparable to graphite, whereas those grown by catalytic decomposition have many more defects and hence a lower Young’s modulus. The strong carbon-carbon bonds within each layer characterize well-graphitized nanotubes, while the interactions between layers are weak. TEM images of CVD grown nanotubes indeed reveal that the carbon sheets are neither continuous nor parallel to the tube axis.

Yu et al. [94] have developed and built a manipulation tool that can also be used as a mechanical loading device, which operates inside a SEM. Individual MWCNT were picked up and then attached at each end of opposing tips of AFM cantilever probes. Nanotubes were stress-loaded *in situ* in the SEM with observations recorded on video film. Measurement of tensile strength for individual MWCNTs has revealed a “sword-in-sheath” breaking mechanism, similar to that observed for carbon fibres [95]. Tensile strengths of up to 20 GPa were reported for graphite whiskers [96], which were said to have a scroll-like structure rather than the Russian doll structure (nested cylinders) observed in MWCNTs. The tensile strength of the outermost layer ranged from 11 to 63 GPa for a set of 19 MWCNTs. Analysis of the stress-strain curves indicated that the Young’s modulus for this layer varied from 270 to 950 GPa. This work was further extended to measure the strength of individual MWCNTs [96, 97] to SWCNT ropes [98]. They measured the mechanical response of 15 SWCNT ropes under a tensile load and concluded that the force-strain data is well fitted by a model that assumes the load is carried by the SWCNT at the perimeter of each rope. The average tensile strength of SWCNTs in the

perimeter ranged from 13 to 53 GPa, with a mean value of 30 GPa. Based on the same model a Young's modulus ranging from 320 to 1470 GPa, with a mean value of 1002 GPa, was calculated. Multiwalled carbon nanotubes can be bent repeatedly through large angles using the AFM tip without undergoing catastrophic failure, suggesting that nanotubes are remarkably flexible and resilient. Folvo et al. [99] used the "Nanomanipulator" AFM system to produce and record nanotube translations and bends by applying lateral stress at specific locations along the tube. These fascinating mechanical properties of carbon nanotubes can be exploited in applications that might include bullet-proof vests, aircraft brakes and earthquake-resistant buildings, while nanotube tips for scanning probe microscopes are already commercially available.

New composite materials with improved mechanical or electrical properties have been made from carbon nanotubes. However, there are a number of problems to overcome for the efficient use of nanotubes for reinforcement applications. The properties of the nanotubes need to be optimized; in particular, the tubes must be efficiently bonded to the material they are reinforcing (the matrix), in order to maximize load transfer.

6. Applications

By the end of the 1990s, applications of carbon nanotubes and nanofibres were attracting extensive and interdisciplinary research interest. Carbon nanotubes have proven to be good field emitters after Rinzler et al. [16] reported electron emission from a single nanotube. There has recently been extensive research focused upon obtaining a uniform field emission from large-area films of nanotubes or nanofibres [17–20]. Carbon nanotubes have now been used for scanning electron microscope tips [21], as conducting fillers in polymer composite materials [22], and in fuel cell electrodes [23]. It has been proven that carbon nanotubes can be used in nanoelectronics as diodes and transistors [24], in supercapacitors [25], as electromechanical actuators [26], and as chemical sensors [27]. Carbon nanotubes and nanofibres have also found potential applications in the field of biotechnology, e.g. as a cell growth scaffold [28], in DNA microarrays [29], and for protein sensing [30].

The age of semiconductor technology started in 1947, just half a century ago, when the first semiconductor device, a germanium-based transistor, was invented [100]. In 1965 Moore [101] observed an exponential growth in the number of transistors per integrated circuit and predicted that this trend will continue. Since then, the miniaturization of devices has been continuous with exponential growth of the number of transistors, and computers have become faster and smaller. At the present pace of miniaturization, it is expected that the end of the path could however be reached within a decade. In order to overcome this technological limit, several types of devices are being investigated, which make use of quantum effects rather than trying to overcome them. For this reason, the nanometre-scale carbon materials, namely the fullerenes and nanotubes, have attracted great interest in the field of semiconductor technology. In general, there are two kinds of elemental device structures, two-terminal and three-terminal. The transistor is a three-terminal device with a variety of structures, materials, and basic functional mechanisms. A typical two-terminal device is the diode, having also a variety of structures and applications, such as switching, rectification, and solar cells. The first "nanotube nanodevice" reported by Collins et al. [102] was a kind of nanodiode. Semiconducting nanotubes can work as transistors. The tube can be made to conduct (turned ON) by applying a negative bias to the gate, and turned OFF with

positive bias. A negative bias induces holes in the tube and allows it to conduct. Positive biases, on the other hand, deplete the holes and decrease the conductance. The resistance of the OFF state can be more than a million times greater than the ON state. This behaviour is analogous to that of a p-type metal oxide-silicon field effect transistor (MOSFET), except that the nanotube replaces silicon as the material hosting the charge carriers. It has been shown that a field effect transistor (FET) can be made from individual semiconducting single walled nanotubes by Tans et al. [103], and later by Martel et al. [104].

Future interconnects development driven by the demand for high-speed chip transmission was emphasized in the International Technology Roadmap for Semiconductors (ITRS) [105]. Material requirements and difficulties in processing are the challenges in interconnect technology. Decrease of an interconnect's cross section will result in a current density increase; electromigration at high current densities ($> 10^6$ A/cm²) is the problem for common interconnect materials like copper. It will be extremely difficult to achieve the high aspect ratio required in future device interconnects using only conventional semiconducting processing technologies. Carbon nanotubes and less crystalline carbon nanofibres with diameters from a few nanometres up to 100 nm and several microns in length could be an ideal material for nanoelectronic three-dimensional (3D) interconnexions, due to their high aspect ratio, high electrical and thermal conductivities, and good mechanical properties [74, 106]. It was shown that the current carrying capacity of multiwalled CNTs did not degrade after 350 h at a current density of 10^{10} A/cm² at 250 °C [107], which is 100 times more than copper before electromigration occurs. The scattering-free, ballistic transport of electrons in defect-free carbon nanotubes is the most attractive property for the possible use of CNTs as interconnects, although large contact resistance limits the ballistic current-carrying capability of CNTs. Thermal conductivity of the individual MWCNT was measured to be higher than 3000 W/mK, which is greater than diamond and the basal plane of graphite (both 2000 W/mK) [108].

Three-dimensional nano-carbon structures that can transfer the exceptional properties of carbon nanomaterials to meso- and microscale engineering materials are essential for the development of many applications [74]. Tennent et al. [109] at Hyperion Catalysis in 1998 patented a method of preparing 3D microscopic structures by dispersing carbon fibrils (nanotubes or nanofibres) in a medium and separating them from the medium by filtration and evaporation to form a porous mat or sheet. Carbon nanotubes and nanofibres synthesized using CVD are usually in the form of a powder or a thin film on a flat substrate and direct synthesis of 3D carbon nanotube and nanofibre macroscopic structures are still challenging operations.

Well known engineering materials like carbon, ceramic, or glass fibres could be exploited as a support for the formation of 3D nanostructures (Fig. 3). Growth of CNTs and CNFs on the surface of carbon fibres was first reported to improve composite shear strength [110, 111] and load transfer at the fibre/matrix interface [114]. The high surface area of carbon and ceramic fibres coated with nanotubes and nanofibres is important for use in electrochemical applications [113–115]. Jo et al. [116] reported excellent field emission properties of CNTs grown on the surface of carbon fibres in carbon cloth, which could potentially be used in flat panel displays. Boskovic et al. [117] reported low temperature DC PECVD synthesis of carbon nanofibres on the surface of carbon fibres using a Co colloid as catalyst. It was also demonstrated that using the same Co colloid catalyst and the same PECVD method, it is possible to grow carbon nanotubes

and nanofibres on arbitrarily micromachined silicon three-dimensional ‘micrograss’ surfaces [118]. Hart et al. [118] demonstrated that conventional metal deposition techniques can be used to obtain uniform SWCNT and DWCNT film growth by atmospheric pressure thermal CVD on arbitrarily microstructured silicon micrograss surfaces, where the surfaces face the deposition source in any orientation from vertical to horizontal. These principles can be applied to grow a wide variety of nanostructures on microstructures having arbitrary 3D topography, so extending the fabrication capability for hierarchically microstructured and nanostructured substrates.

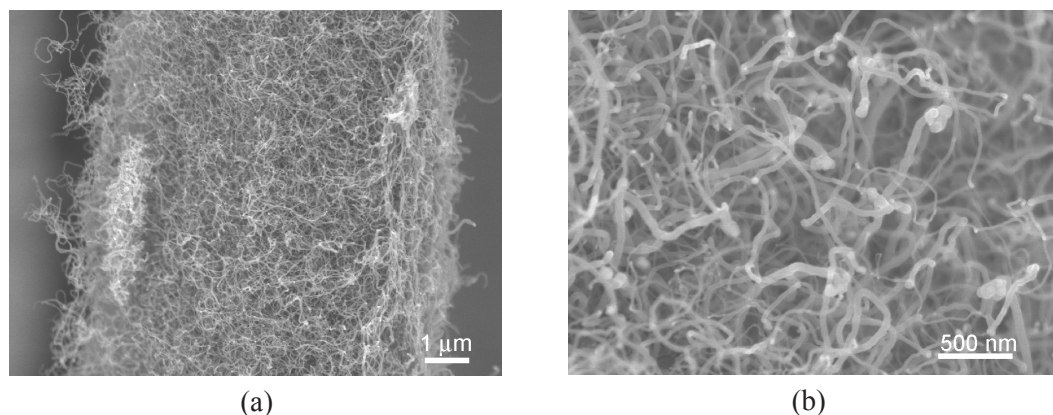


Figure 3. (a) SEM image of carbon nanotubes grown on the surface of a carbon fibre using thermal CVD; (b) enlarged image of the carbon fibre surface showing carbon nanotubes.

Carbon fibre bundles, and woven and non-woven carbon fibre cloth can be used as a three-dimensional scaffold for carbon nanotube synthesis on the surface of carbon fibres and in the empty space between them. Boskovic has found [119] that when the catalyst is impregnated and dispersed within a fibrous matrix (carbon or ceramic fibre cloth or felt), rather than being left on the surface, more efficient deposition of nanofibres and/or nanotubes results. Carbon nanotubes and nanofibres were grown using an ethylene and hydrogen mixture at 650 °C. The nanotubes/nanofibres are produced in clumps originating from the surface of the catalyst particles. The amount of produced carbon nanomaterials could be controlled through variation of catalyst loading.

Veedu et al. [120] reported that well-aligned CNTs grown perpendicular to a two-dimensional (2D) woven fabric of SiC fibres improved the mechanical and thermal properties significantly. Interlaminar fracture-toughness of the resulting 3D composite has shown an improvement of 350% compared with the base composite without CNTs. The interlaminar shear sliding fracture toughness was improved by about 54%. It was also reported that the addition of carbon nanotubes has significantly improved dissipation of vibration energy under cyclic loading and damping (514%). The coefficient of thermal expansion was reduced to 38% of the original value and thermal conductivity was improved by 51%.

Three-dimensional composite materials containing carbon nanotubes and carbon fibres are a good candidate for many potential applications. The high thermal conductivity of these materials may be of use in automotive and aerospace applications and for heat distribution or hotspot control. The first attempts to develop carbon-carbon composites containing carbon

nanotubes have already been reported in the literature [121, 122]. The high electrical conductivity of these materials could be used, for example, in electronic components packaging, as gas diffusion layers in fuel cells or in electromagnetic shielding. Carbon fabric impregnated with carbon nanotubes could be used for many applications such as lightweight structures, brake discs and bullet-proof vests.

7. Conclusions

Carbon nanotube- and nanofibre-related research has led to the development of new production routes and the suggestion and realization of many fascinating applications, and it is growing rapidly around the world.

The combination of CNTs' electronic properties and dimensions makes them ideal building blocks for future electronic devices and circuits. Integration of techniques for CNT growth on specified locations using PECVD in conventional semiconducting processing could provide the first step towards exploitation of these CNT properties. However, this top-down approach could be replaced with a bottom-up approach where the molecular properties of CNT will be exploited as a necessary requirement for high device density architectures. Self-assembly of CNTs into functional devices based on molecular recognition could be a promising approach for future large-scale integrated circuits. The nanometre dimensions of CNTs and their high current-carrying capacity, together with the possibility for ballistic electron transport, are ideal properties for interconnect applications in the electronics industry. The main challenge for large-scale production is good electrical coupling of the nanotubes to the contacts. Controlled, reproducible and low cost production of SWCNTs and the separation of metallic and semiconducting tubes are the main requirements for further advances towards large scale production of CNT-based electronics. Metallic SWCNTs could function as interconnects, while semiconducting SWCNTs could perform as nanoscale transistors.

Chemical vapour deposition has proven to be an effective technique for the synthesis of carbon nanomaterials and nanostructures. It is widely accepted in both the academic and industrial communities as a cost-effective and scalable method that gives control over the synthesis of nanomaterials on various substrates, including 3D ones. Chemical vapour deposition offers controlled carbon nanomaterial and nanostructure fabrication that is easily scalable and adoptable for mass production at an industrial level.

Carbon nanotube and nanofibre composites have already reached the market with the first sports applications including tennis rackets, baseball bats, and racing bicycles. It is expected that carbon nanotube composite materials will have many more applications, including automotive and aerospace components (including brakes) and structures.

Intensive research in recent decades has already set up solid foundations for exploitation of the fascinating properties of carbon nanomaterials for the benefit of humanity. Significant advances in understanding, synthesis and applications of carbon nanomaterials are however still ahead of us.

Acknowledgments

I would like to thank my colleagues Prof John Robertson, Prof Alan Windle, Dr Krzysztof Koziol, Alfred Chuang and Dr Ian Kinloch for inspiration and their contribution to the nanotube

and nanofibre work that I conducted at the University of Cambridge. I am also very grateful to my colleagues from Dunlop Aerospace: Ron, Judith, Paris, Neil, Craig, Lynda, Dave and Toby for reading the manuscript draft and giving me valuable suggestions for improving it.

References

1. T.V. Hughes, and C.R. Chambers, U.S. Patent No. 405480, 18th June 1889.
2. P. Schützenberger and L. Schützenberger, *C.R. Acad. Sci.* **111** (1890) 774.
3. L.V. Radushkevich and V.M. Luk'yanovich, *Zh. Fiz. Khim.* **26** (1952) 88.
4. W.R. Davis, R.J. Slawson and G.R. Rigby, *Nature* **171** (1953) 756.
5. R.T.K. Baker and J.J. Chludzinski, *J. Catal.* **64** (1980) 464.
6. H.W. Kroto, J.H. Heath, S.C. O'Brien, R.F. Curl and R.E. Smalley, *Nature* **318** (1985) 162.
7. S. Iijima, *Nature* **354** (1991) 56.
8. S. Iijima and T. Ichihashi, *Nature* **363** (1993) 603.
9. D.S. Bethune, C.H. Kiang, M.S. de Vries, G. Gorman, R. Savoy, J. Vazquez and R. Beyers, *Nature* **363** (1993) 605.
10. T.W. Ebbesen and P.M. Ajayan, *Nature* **358** (1992) 220.
11. A. Thess, R. Lee, P. Nikolaev, H. Dai, P. Petit, J. Robert, C. Xu, Y.H. Lee, S.G. Kim, D.T. Colbert, G. Scuseria, D. Tomanek, J.E. Fisher and R.E. Smalley, *Science* **273** (1996) 483.
12. A.M. Rao, E. Richter, S. Bandow, B. Chase, P.C. Eklund, K.A. Williams, S. Fang, K.R. Subbaswamy, M. Menon, A. Thess, R.E. Smalley, G. Dresselhaus and M.S. Dresselhaus, *Science* **275** (1997) 187.
13. Z.Ja. Kozavskaja, L.A. Chernozatonskii and E.A. Federov, *Nature* **359** (1992) 670.
14. D. Laplaze, P. Bernuer, W.R. Maser, G. Flament and T. Guillard, *Carbon* **36** (1998) 681.
15. S. Amelinckx, X.B. Zhang, D. Bernaerts, X.F. Zhang, V. Ivanov and J.B. Nagy, *Science* **265** (1994) 635.
16. A.G. Rinzler, J.H. Hafner, P. Nikolaev, L. Lou, S.G. Kim, D. Tomanek, P. Nordlander, D.T. Colbert and R.E. Smalley, *Science* **269** (1995) 1550.
17. Z.F. Ren, Z.P. Huang, J.W. Xu, J.H. Wang, P. Bush, M.P. Siegal and P.N. Provencio, *Science* **282** (1998) 1105.
18. X. Xu and G.R. Brandes, *Appl. Phys. Lett.* **74** (1999) 2549.
19. D. Xu, G. Guo, L. Gui, Y. Tang, Z. Shi, Z. Jin, Z. Gu, W. Liu, X. Li and G. Zhang, *Appl. Phys. Lett.* **75** (1999) 481.
20. C.J. Lee, D.W. Kim, T.J. Lee, Y.C. Choi, Y.S. Park, W.S. Kim, Y.H. Lee, W.B. Choi, N.S. Lee, J.M. Kim, Y.G. Choi and S.C. Yu, *Appl. Phys. Lett.* **75** (1999) 1721.
21. H. Dai, J.H. Hafner, A.G. Rinzler, D.T. Colbert and R.E. Smalley, *Nature* **384** (1996) 147.
22. S.A. Curran, P.M. Ajayan, W.J. Blau, D.L. Carroll, J.N. Coleman, A.B. Dalton, A.P. Davey, A. Drury, B. McCarthy, S. Maier and A.A. Strevens, *Adv. Mater.* **10** (1998) 1091.
23. A.C. Dillon, K.M. Jones, T.A. Bekkedahl, C.H. Kiang, D.S. Bethune and M.J. Heben, *Nature* **386** (1997) 377.
24. S.J. Tans, A.R.M. Verschueren and C. Dekker, *Nature* **393** (1998) 49.
25. C. Niu, E.K. Sichel, R. Hoch, D. Moy and H. Tennent, *Appl. Phys. Lett.* **70** (1997) 1480.
26. R.H. Baughman, C. Cui, A.A. Zakhidov, Z. Iqbal, J.N. Barisci, G.M. Spinks, G.G. Wallace, A. Mazzoldi, D. Rossi, A.G. Rinzler, O. Jaschinski, S. Roth and M. Kertesz, *Science* **284** (1999) 1340.
27. J. Kong, N.R. Franklin, C. Zhou, M.G. Chaplene, S. Peng, K. Cho and H. Dai, *Science* **287** (2000) 622.
28. L.P. Zanello, B. Zhao, H. Hu and R.C. Haddon, *Nano Lett.* **6** (2006) 562.
29. J.E. Koehne, H. Chen, A.M. Cassell, Q. Yi, J. Han, M. Meyyappan and J. Li, *Clin. Chem.* **50** (2004) 1886.
30. R.J. Chen, H.C. Choi, S. Bangsaruntip, E. Yenilmez, X.W. Tang, Q. Wang, Y.L. Chang and H.J. Dai,

- J. Am. Chem. Soc.* **126** (2004) 1563.
31. P.M. Ajayan and S. Iijima, *Nature* **358** (1992) 23.
 32. M.S. Dresselhaus, G. Dresselhouse and P.C. Eklund, "Science of Fullerenes and Carbon Nanotubes", Academic Press, Oxford, 1996.
 33. L.F. Sun, S.S. Xie, W. Liu, W.Y. Zhou, Z.Q. Liu, D.S. Tang, G. Wang and L.X. Qian, *Nature* **403** (2000) 384.
 34. L.-C. Qin, X. Zhao, K. Hirahara, Y. Miyamoto, Y. Ando and S. Iijima, *Nature* **408** (2000) 50.
 35. N. Wang, Z.K. Tang, G.D. Li and J.S. Chen, *Nature* **408** (2000) 50.
 36. T. Baird, J.R. Fryer and B. Grant, *Carbon* **12** (1974) 591.
 37. T. Baird, J.R. Fryer and B. Grant, *Nature* **233** (1971) 329.
 38. N.M. Rodriguez, A. Chambres and R.T.K. Baker, *Langmuir* **11** (1995) 3862.
 39. S. Motojima, M. Kawaguchi, K. Nozaki and H. Iwanaga, *Appl. Phys. Lett.* **56** (1990) 321.
 40. C.A. Bernardo, I. Alstrup and J.R. Rostrup-Nielsen, *J. Catal.* **96** (1985) 517.
 41. A. Thess, R. Lee, P. Nikolaev, H. Dai, P. Petit, J. Robert, C. Xu, Y.H. Lee, S.G. Kim, A.G. Rinzler, D.T. Colbert, G.E. Scuseria, D. Tomanek, J.E. Fisher and R.E. Smalley, *Science* **273** (1996) 483.
 42. H.M. Cheng, F. Li, X. Sun, S.D.M. Brown, M.A. Pimenta, A. Marucci, G. Dresselhaus and M.S. Dresselhaus, *Chem. Phys. Lett.* **289** (1998) 602.
 43. A.B. Dalton, S. Collins, E. Munoz, J.M. Razal, V.H. Ebron, J.P. Ferraris, J.N. Coleman, B.G. Kim and R.H. Baughman, *Nature* **423** (2003) 703.
 44. V.A. Davis, L.M. Ericson, A.N.G Parra-Vasquez, H. Fan, Y.H. Wang, V. Prieto, J.A. Longoria, S. Ramesh, R.K. Saini, C. Kittrell, W.E. Billups, W.W. Adams, R.H. Hauge, R.E. Smalley and M. Pasquali, *Macromol.* **37** (2004) 154.
 45. M. Zhang, K.R. Atkinson and R.H. Baughman, *Science* **306** (2004) 1358.
 46. Y.-L. Li, I.A. Kinloch and A.H. Windle, *Science* **304** (2004) 276.
 47. R.T.K. Baker and P.S. Harris, *Chem. Phys. Carbon* **14** (1978) 1.
 48. M. Yose-Yacaman, M. Miki-Yoshida, L. Rendon and J.G. Santiesteban, *Appl. Phys. Lett.* **62** (1993) 657.
 49. P.M. Ajayan and S. Iijima, *Nature* **361** 33 (1993).
 50. A.M. Rao, E. Richer, S. Bandow, B. Chase, P.C. Eklund, K.A. Williams, S. Fang, K.R. Subbaswamy, M. Menon, A. Thess, R.E. Smalley, G. Dresselhaus and M.S. Dresselhaus, *Science* **275** (1997) 187.
 51. J. Kong, A.M. Cassell and H.J. Dai, *Chem. Phys. Lett.* **292** 567 (1998).
 52. N.M. Rodriguez, *J. Mater. Res.* **8** 3233 (1993).
 53. C.E. Snyder, M.W. Mandeville, H.G. Tennent, L.K. Truesdale and J.J. Barber, Carbon Fibrils, Hyperion Catalysis International, WO8907163A1, 10th August 1989.
 54. C. Singh, M.S.P. Shaffer, K.K.K. Koziol, I.A. Kinloch and A.H. Windle, *Chem. Phys. Lett.* **372** (2003) 860.
 55. L.C. Qin, D. Zhou, A.R. Krauss and D.M. Gruen, *Appl. Phys. Lett.* **72** (1998) 3437.
 56. S.H. Tsai, C.W. Chao, C.L. Lee and H.C. Shih, *Appl. Phys. Lett.* **74** (1999) 3462.
 57. Y.C. Choi et al., *Appl. Phys. Lett.* **76** (2000) 2367.
 58. C. Bower, W. Zhu, S. Jin and O. Zhou, *Appl. Phys. Lett.* **77** (2000) 830.
 59. M. Okai, T. Muneyoshi, T. Yaguchi and S. Sasaki, *Appl. Phys. Lett.* **77** (2000) 3468.
 60. V.I. Merkulov, D.H. Lowndes, Y.Y. Wei, G. Eres and E. Voelkl, *Appl. Phys. Lett.* **76** (2000) 1534.
 61. M. Chhowalla et al., *J. Appl. Phys.* **90** (2001) 5308.
 62. J. Li, R. Stevens, L. Delzeit, H.T. Ng, A. Cassell, J. Han and M. Meyyappan, 2002 *Appl. Phys. Lett.* **81** (2002) 910.
 63. L. Delzeit, I. McAninch, B.A. Cruden, D. Hash, B. Chen, J. Han and M. Meyyappan, *J. Appl. Phys.* **91** (2002) 6027.

64. Y.H. Wang, J. Lin, C.H.A. Huan and G.S. Chen, *Appl. Phys. Lett.* **79** (2001) 680.
65. B.O. Boskovic, V. Stolojan, R.U. Khan, S. Haq and S.R.P. Silva, *Nature Materials* **1** (2002) 165.
66. O.-J. Lee and K.-H. Lee *Appl. Phys. Lett.* **82** (2003) 3770.
67. K.B.K. Teo et al., *Appl. Phys. Lett.* **79** (2001) 1534.
68. S. Hofmann, C. Ducati, B. Kleinsorge and J. Robertson, *Appl. Phys. Lett.* **83** (2003) 135.
69. S. Hofmann, C. Ducati, B. Kleinsorge and J. Robertson, *Appl. Phys. Lett.* **83** (2003) 4661.
70. R.T.K. Baker, M.A. Barber, P.S. Harris, F.S. Feates and R.J. Waite, *J. Catal.* **26** (1972) 51.
71. R.T.K. Baker and R.J. Waite, *J. Catal.* **37** (1975) 101.
72. A. Oberlin, M. Endo and T. Koyama, *J. Cryst. Growth* **32** (1976) 335.
73. S. Helveg, C. Lopez-Cartes, J. Sehested, P.L. Hansen, B.S. Clausen, J.R. Rostup Nielsen, F. Abil-Pedersen and J.K. Nørskov, *Nature* **427** (2004) 426.
74. R.H. Baughman, A.A. Zakhidov and W.A. de Heer, *Science* **297** (2002) 787.
75. L. Chico et al., *Phys. Rev. Lett.* **76** (1996) 971.
76. H. Dai, E.W. Wong and C.M. Lieber, *Science* **272** (1996) 523.
77. T.W. Ebbesen, H.J. Lezec, H. Hiura, J.W. Bennett, H.F. Ghaemi and T. Thio, *Nature* **382** (1996) 54.
78. S.J. Tans, M.H. Devoret, H. Dai, A. Thess, R.E. Smalley, L.J. Geerlings and C. Dekker, *Nature* **386** (1997) 474.
79. S. Frank, P. Poncharal, Z.L. Wang and W. de Heer, *Science* **280** (1998) 1744.
80. P.L. McEuen, M. Bockrath, D.H. Cobden, Y.-G. Yoon and S.G. Louie, *Phys. Rev. Lett.* **83** (1999) 5098.
81. M. Bockrath, D.H. Cobden, P.L. McEuen, N.G. Chopra, A. Zentl, A. Thess and R.E. Smalley, *Science* **275** (1997) 1922.
82. S.J. Tans, M.H. Devoret, R.J.A. Groeneveld and C. Dekker, *Nature* **394** (1998) 761.
83. L.C. Venema et al., *Science* **283** (1999) 52.
84. A. Bachtold, C. Strunk, J.-P. Salvetat, J.-M. Bonard, L. Forro, T. Nussbaumer and C. Schönenberger, *Nature* **397** (1999) 673.
85. K. Tsukagoshi, B.W. Alphenaar and H. Ago, *Nature* **401** (1999) 572.
86. J. Nygard, D.H. Cobden and P.E. Lindelof, *Nature* **408** (2000) 342.
87. W. Liang, M. Bockrath, D. Bozovic, J.H. Hafner, M. Tinkham and H. Park, *Nature* **411** (2001) 665.
88. A. Javey, J. Guo, Q. Wang, M. Lundstrom and H. Dai, *Nature* **424** (2003) 654.
89. C.T. White and T.N. Todorov, *Nature* **393** (1998) 240.
90. D.J. Thouless, *Phys. Rev. Lett.* **39** (1977) 1167.
91. D.T. Colbert et al., *Science* **266** (1994) 1218.
92. M.M.J. Treacy, T.W. Ebbesen and J.M. Gibson, *Nature* **381** (1996) 678.
93. J.-P. Salvetat et al., *Adv. Mat.* **11** (1999) 161; *Phys. Rev. Lett.* **82** (1999) 944.
94. M. Yu, O. Lourie, M.J. Dryer, K. Molini, T.F. Kelly and R.S. Ruoff, *Science* **278** (2000) 637.
95. G.G. Tibbets and C.P. Beetz, *J. Phys. D Appl. Phys.* **20** (1987) 292.
96. R. Bacon, *J. Appl. Phys.* **31** (1959) 283.
97. M. Yu, B.I. Yakobson and R. Ruoff, *J. Phys. Chem. B* **104** (2000) 8764.
98. M. Yu, B.S. Files, S. Arepalli and R.S. Ruoff, *Phys. Rev. Lett.* **84** (2000) 5552.
99. M.R. Falvo, G.J. Clary, R.M. Taylor II, V. Chi, V.P. Brooks Jr, S. Washburn and R. Superfine, *Nature* **389** (1997) 582.
100. S. Saito, *Science* **278** (1997) 77.
101. G.E. Moore, *Electronics* **38** (1965) 114.
102. P.G. Collins, A. Zehl, H. Brando, A. Thess and R.E. Smalley, *Science* **278** (1997) 100.

103. S.J. Tans, A.R.M. Verschueren and C. Dekker, *Nature* **393** (1998) 49.
104. R. Martel, T. Schmidt, H.R. Shea, T. Hertel and Ph. Avouris, *Appl. Phys. Lett.* **73** (1998) 2447.
105. International Technology Roadmap for Semiconductors (Semiconductor Industry Association, San Jose, CA, 2003); <http://public.itrs.net/>
106. "Carbon Nanotubes: Synthesis, Structure, Properties and Applications" (M.S. Dresselhaus, G. Dresselhouse and P. Avouris, eds.) Springer, New York, 2001.
107. B.Q. Wei, R. Vajtai and P.M. Ajayan, *Appl. Phys. Lett.* **79** (2001) 1172.
108. P. Kim, L. Shi, M. Majumdar and P.L. McEuen, *Phys. Rev. Lett.* **87** (2001) 215502.
109. H. Tennent, R.W. Hausslein, N. Leventis and D. Moy, Hyperion Catalysis International, Inc., Patent U.S. 5,846,658, 8th December 1998.
110. W.B. Downs and R.T.K. Baker, *Carbon* **29** (1991) 1173.
111. W.B. Downs and R.T.K. Baker, *J. Mater. Res.* **10** (1995) 625.
112. E.T. Thostenson, W.Z. Li, D.Z. Wang, Z.F. Ren and T.W. Chou, *J. Appl. Phys.* **91** (2002) 6034.
113. X. Sun, R. Li, D. Villers, J.P. Dodelet and S. Desilets, *Chem. Phys. Lett.* **379** (2003) 99.
114. C. Wang, M. Waje, X. Wang, J. Tang, R.C. Haddon and Y. Yan, *Nano Lett.* **4** (2004) 345.
115. M.A. Marphy, G.D. Wilcox, R.H. Dahm and F. Marken, *Electrochem. Comm.* **5** (2003) 51.
116. S.H. Jo, D.Z. Wang, J.Y. Huang, W.Z. Li, K. Kempa and Z.F. Ren, *Appl. Phys. Lett.* **85** (2004) 810.
117. B.O. Boskovic, V. Golovko, M. Cantoro, B. Kleinsorge, C. Ducati, A.T.H. Chuang, S. Hofmann, J. Robertson and B.F.G. Johnson, *Carbon* **43** (2005) 2643.
118. A.J. Hart, B.O. Boskovic, A.T.H. Chuang, V.B. Golovko, J. Robertson, B.F.G. Johnson and A.H. Slocum, *Nanotechnol.* **17** (2006) 1397.
119. B.O. Boskovic, The Morgan Crucible Company Plc, WO 2004078649, 16th September 2004.
120. V.P. Veedu, A. Cao, X. Li, K. Ma, C. Soldano, S. Kar, P.M. Ajayan and M.N. Ghasemi-Nejhad, *Nature Materials* **5** (2006) 458.
121. D.-S. Lim, J.-W. An and H.J. Lee, *Wear* **252** (2006) 512.
122. X. Li, K. Li, H. Li, J. Wei and C. Wang, *Carbon* **45** (2007) 1662.